

**Wavelet methods in the relativistic three-body problem**

Fatih Bulut and W. N. Polyzou\*

*Department of Physics and Astronomy, The University of Iowa, Iowa City, Iowa 52242, USA*

(Received 27 July 2005; published 27 February 2006)

We discuss the use of wavelet bases to solve the relativistic three-body problem in momentum space. We address the treatment of the moving singularities that appear in the relativistic three-body problem. Wavelet bases can be used to transform momentum-space scattering integral equations into an approximate system of linear equations with a sparse matrix. This has the potential to reduce the size of realistic three-body calculations with minimal loss of accuracy. The wavelet method leads to a clean interaction-independent treatment of the scattering singularities that does not require any subtractions.

DOI: [10.1103/PhysRevC.73.024003](https://doi.org/10.1103/PhysRevC.73.024003)

PACS number(s): 21.45.+v, 11.80.-m, 24.10.Jv, 25.10.+s

**I. INTRODUCTION**

This is the third paper [1,2] in a series of investigations designed to explore the potential advantages of using wavelet numerical analysis to solve scattering problems. Our long-term goal is to apply these methods to solve the relativistic three-body problem.

Commercially, wavelets are used to convert raw digitized photographic images to compressed JPEG files [3]. In this application the data compression leads to a large savings in storage space with a minimal loss of information. The compression involves expanding the raw digital image in a wavelet basis and setting the smaller expansion coefficients to zero. The kernel of a scattering integral equation and a raw digital image can both be approximated by rectangular arrays of numbers that describe structures with several scales. This suggests that the bases used to compress digital images could be used to generate accurate sparse-matrix approximations to the kernel.

The ability to construct numerically exact solutions to the quantum-mechanical three-body problem coupled with the ability to accurately measure complete sets of experimental observables constrains the form of the three-nucleon Hamiltonian. These constraints have resulted in the construction of realistic model nucleon-nucleon interactions [4–6]. When these interactions are used in the many-nucleon Hamiltonian, the resulting dynamical model provides a good quantitative description of low-energy nuclear physics [7].

The state of the art in few-body computations has improved to the point where numerically exact scattering calculations at energy and momentum transfers of hundreds of mega-electronvolts have been performed [8]. Higher-energy calculations are possible. As in the low-energy case, for higher-energy reactions the structure of Hamiltonians can be constrained by the consistency of the few-body calculations with precise measurements of complete sets of experimental observables.

The success of the few-body approach to low-energy nuclear physics is a consequence of (1) knowing the relevant degrees of freedom (nucleons), (2) working with the most general Hamiltonians involving these degrees of freedom that are consistent with the symmetries of the system

(Galilean invariance), and (3) understanding the relation between the few- and the many-body problems (cluster properties). To extend this success to reactions involving higher-energy scales, (1) the relevant degrees of freedom may have to include explicit mesonic or subnucleonic degrees of freedom, (2) Galilean invariance must be replaced with Poincaré invariance, and (3) cluster properties must be maintained.

Each of the required extensions of low-energy nuclear dynamics is nontrivial, and progress has been made on all three problems [8–13]. The purpose of this paper is to focus on how to use wavelet numerical analysis to treat the type of moving singularities that appear in the Poincaré invariant three-body problem. Although the scope of this paper is limited to three-nucleon models with no explicit mesonic or subnucleonic degrees of freedom and  $S$ -matrix cluster properties [14], the formulation and advantage of methods discussed in this paper are straightforward to extend to systems with explicit mesonic degrees of freedom and stronger forms of cluster properties [13]. These methods can also be used to solve the nonrelativistic three-body problem. Moving singularities are a generic feature of the dynamical equations in all of these cases.

Relativistic few-body equations are naturally formulated in momentum space. Relativistic kinematic factors, Wigner rotations, and Melosh rotations are all multiplication operators in momentum space. The compactness of the iterated Faddeev-Lovelace kernel implies that the kernel of the integral equations can be uniformly approximated by a finite matrix, resulting in a finite linear system. In the momentum representation these linear systems have large dense matrices, which increase in size with increasing energy and momentum transfer. It is desirable to be able to perform accurate calculations at energy and momentum scales at which subnuclear degrees of freedom are relevant. At these scales a relativistic treatment is required and advances in computational efficiency are needed to perform realistic calculations. The ability of the wavelet transform to efficiently transform a dense matrix to an approximate sparse matrix suggests that wavelet methods can provide a powerful tool for improving the efficiency of both relativistic and nonrelativistic few-body computations.

The advantages of using wavelet numerical analysis to solve momentum-space scattering integral equations were investigated in Refs. [1,2]. These papers used wavelet numerical

\*Electronic address: [polyzou@uiowa.edu](mailto:polyzou@uiowa.edu)

analysis to solve the Lippmann-Schwinger equation for a system of two nucleons interacting with a Malfliet Tjon  $V$  potential [15,16] by use of partial-wave expansions [1] and direct integration [2]. In both applications the kernel of the integral equation was accurately approximated by a sparse matrix, which resulted in accurate approximate solutions. The success of these applications indicates that wavelet numerical analysis will have similar advantages when applied to the relativistic three-body problem.

The feature of the three-body problem that is not present in the two-body applications is moving singularities. The method used to treat fixed singularities in Refs. [1,2] is not applicable to problems with moving singularities. The purpose of this paper is to illustrate how to apply wavelet numerical analysis to treat the type of moving singularities that appear in the relativistic three-body problem.

**II. OVERVIEW—WAVELET NUMERICAL ANALYSIS**

In this section we give a brief introduction to the use of wavelets in scattering calculations. This is because few-body scattering problems require a specialized application of wavelets that is not discussed extensively in the literature.

The applications in Refs. [1,2] used Daubechies' wavelets. The Daubechies' wavelets are orthonormal basis functions with compact support, and the results of Refs. [1,2] indicate that the Daubechies' wavelets are suitable for scattering calculations.

Daubechies' wavelets [17,18] are discussed in many texts on wavelets [19–22]. They are fractal functions that have complex structures on all scales. Because the basis functions have structure on all scales, numerical applications with wavelets require a different approach to numerical analysis; hence we use the term wavelet numerical analysis.

We use the Daubechies' wavelets because they are a dense orthonormal set of compactly supported functions with the property that finite linear combinations can locally pointwise represent low-degree polynomials.

Wavelet bases are generated from two functions by use of translations and unitary scale transformations. These functions are called the scaling function and the mother wavelet. The scaling function  $\phi(x)$  is the solution of the linear renormalization group equation:

$$D\phi(x) = \sum_{l=0}^{2K-1} h_l T^l \phi(x), \tag{1}$$

with normalization

$$\int_{-\infty}^{\infty} \phi(x) dx = 1. \tag{2}$$

Equation (1) is called the scaling equation.

In Eq. (1)  $D$  is the unitary scaling operator,

$$Df(x) \equiv \frac{1}{\sqrt{2}} f\left(\frac{x}{2}\right), \tag{3}$$

which stretches the support of the function by a factor of 2. The operator  $T$  is the unitary unit translation operator:

$$Tf(x) = f(x - 1). \tag{4}$$

TABLE I. Daubechies'  $K = 3$  scaling coefficients.

$h_l$	$K = 3$
$h_0$	$(1 + \sqrt{10} + \sqrt{5 + 2\sqrt{10}})/16\sqrt{2}$
$h_1$	$(5 + \sqrt{10} + 3\sqrt{5 + 2\sqrt{10}})/16\sqrt{2}$
$h_2$	$(10 - 2\sqrt{10} + 2\sqrt{5 + 2\sqrt{10}})/16\sqrt{2}$
$h_3$	$(10 - 2\sqrt{10} - 2\sqrt{5 + 2\sqrt{10}})/16\sqrt{2}$
$h_4$	$(5 + \sqrt{10} - 3\sqrt{5 + 2\sqrt{10}})/16\sqrt{2}$
$h_5$	$(1 + \sqrt{10} - \sqrt{5 + 2\sqrt{10}})/16\sqrt{2}$

The coefficients  $h_l$  are real numbers that determine the properties of the scaling function.  $K$  is a positive integer. The calculations in Refs. [1,2] used Daubechies'  $K = 3$  wavelets. The reason for this choice is discussed later. For the  $K = 3$  Daubechies' wavelets, the six scaling coefficients  $h_l$  are given in Table I.

The fractal structure of  $\phi(x)$  is a consequence of Eq. (1) that shows that the scaling function on a given scale is a finite linear combination of translates of the same function on half the scale.

The scaling equation implies that the scaling coefficients  $h_l$  satisfy

$$\sum_{l=0}^{2K-1} h_l = \sqrt{2}, \tag{5}$$

and the solution  $\phi(x)$  of Eq. (1) has support on the interval  $[0, 2K - 1]$  [23].

The unit translates of the scaling function are orthonormal,

$$(T^m \phi, T^n \phi) = \delta_{mn}, \tag{6}$$

provided the scaling coefficients satisfy the additional constraints

$$\sum_{l=0}^{2K-1} h_l h_{l-2m} = \delta_{m0}. \tag{7}$$

The scaling function  $\phi(x)$  is continuous (for  $K > 1$ ) and can be computed exactly at all dyadic rationals by use of Eqs. (1) and (2). This method is used to compute the Daubechies'  $K = 3$  scaling function plotted in Fig. 1.

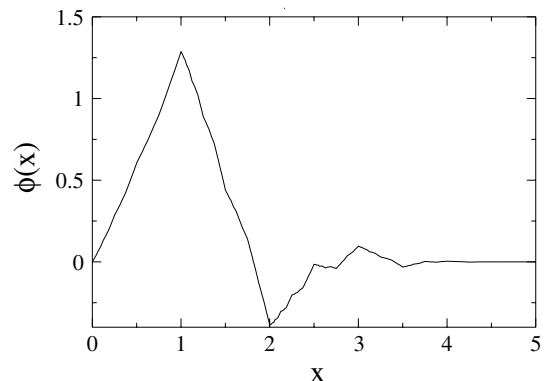


FIG. 1. Daubechies'  $K = 3$  scaling function.

The subspace of square integrable functions on the real line that is spanned by integer translates of the scaling function  $T^n\phi(x)$  is the subspace  $\mathcal{V}_0$ :

$$\mathcal{V}_0 \equiv \left\{ f(x) = \sum_{n=-\infty}^{\infty} f_n T^n \phi(x) \mid \sum_{n=-\infty}^{\infty} |f_n|^2 < \infty \right\}. \quad (8)$$

Application of powers of the scaling operator  $D^k$  to  $\mathcal{V}_0$  defines subspaces  $\mathcal{V}_k$  with coarser resolution ( $k > 0$ ) or finer resolution ( $k < 0$ ):

$$\mathcal{V}_k \equiv D^k \mathcal{V}_0. \quad (9)$$

We call the space  $\mathcal{V}_k$  the approximation space with resolution  $k$ . The resolution determines the size of the smallest features that can be approximated by functions in  $\mathcal{V}_k$ .

The scaling functions

$$\phi_{kn}(x) \equiv D^k T^n \phi(x) = \frac{1}{2^{k/2}} \phi\left(\frac{x}{2^k} - n\right) \quad (10)$$

are an orthonormal basis for  $\mathcal{V}_k$ . The support of  $\phi_{kn}(x)$  is  $[2^k n, 2^k(n + 2K - 1)]$ .

The scaling equation implies the inclusions

$$\mathcal{V}_k \supset \mathcal{V}_{k+1}. \quad (11)$$

The orthogonal compliment of  $\mathcal{V}_{k+1}$  in  $\mathcal{V}_k$  is denoted by  $\mathcal{W}_{k+1}$ :

$$\mathcal{V}_k = \mathcal{V}_{k+1} \oplus \mathcal{W}_{k+1}. \quad (12)$$

Orthonormal basis functions  $\psi_{kn}(x)$  for the subspaces  $\mathcal{W}_k$  are elements of  $\mathcal{V}_{k-1}$  defined by

$$\psi_{kn}(x) = D^k T^n \psi(x), \quad (13)$$

$$\psi(x) = \sum_{l=0}^{2K-1} g_l D^{-1} T^l \phi(x), \quad (14)$$

where

$$g_l = (-)^l h_{2K-l-1}. \quad (15)$$

The subspaces  $\mathcal{W}_k$  are called the wavelet spaces, and the basis functions  $\psi_{kn}$  are called wavelets. The support of  $\psi_{kn}(x)$  is identical to the support of  $\phi_{kn}(x)$ . Because the wavelets are finite linear combinations scaling functions, they are also fractal functions.

The function  $\psi(x) = \psi_{00}(x)$  is called the mother wavelet; the Daubechies'  $K = 3$  mother wavelet is shown in Fig. 2.

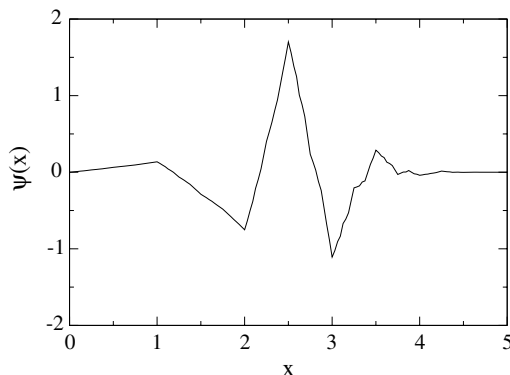


FIG. 2. Daubechies'  $K = 3$  mother wavelet.

The coefficients  $h_l$  for the Daubechies'  $K$  wavelets are determined by Eqs. (5) and (7) and the requirement that the mother wavelet be locally orthogonal to low-degree polynomials:

$$\int_{-\infty}^{\infty} \psi(x) x^n dx = 0; \quad n = 0, 1, \dots, K - 1. \quad (16)$$

It follows that  $\psi_{km}(x)$  is locally orthogonal to all polynomials of degree  $K - 1$ . Equation (16) can be expressed directly in terms of the scaling coefficients:

$$\sum_{l=0}^{2K-1} l^k g_l = \sum_{l=0}^{2K-1} l^k (-)^l h_{2K-1-l} = 0, \quad k = 0 \dots K - 1. \quad (17)$$

For any  $K > 0$ , conditions (5), (7), and (17) determine the coefficients  $h_l$  up to reflection:

$$h_l \rightarrow h'_l \equiv h_{2K-1-l}. \quad (18)$$

The entries in Table I are the solutions of these equations for  $K = 3$ . The Daubechies' wavelets have the property that, as  $k \rightarrow -\infty$  (infinitely fine resolution), the space  $\mathcal{V}_k$  becomes all of  $L^2(\mathbb{R})$ .

Decomposition (12) implies that

$$\mathcal{V}_k = \mathcal{W}_{k+1} \oplus \mathcal{W}_{k+2} \dots \mathcal{W}_{k+m-1} \oplus \mathcal{W}_{k+m} \oplus \mathcal{V}_{k+m} \quad (19)$$

for any  $m > 0$ . The identification of these spaces means that functions in the approximation space  $\mathcal{V}_k$  can be expanded as linear combinations of the scaling basis functions of resolution  $k$  or equivalently as linear combinations of the scaling basis functions of a coarser resolution  $k' = k + m$  and wavelet basis functions of all resolutions from  $k + 1$  to  $k + m$ . The orthogonal transformation that relates these orthonormal bases is called the wavelet transform. For  $N$  basis elements, the wavelet transform can be computed in  $O(N)$  steps, which is faster than a fast Fourier transform.

If  $k \rightarrow -\infty$  with  $l = m + k$  finite, equivalence (19) means that the basis functions on the right-hand side of Eq. (19) become a basis for  $L^2(\mathbb{R})$ . Because the wavelet basis functions  $\psi_{kn}(x)$  are locally orthogonal to degree  $K - 1$  polynomials and only a finite number of the scaling basis functions  $\phi_{ln}(x)$  are nonzero at any  $x$ , it follows that finite linear combinations of  $\phi_{ln}(x)$  must be able to locally pointwise represent degree  $K - 1$  polynomials. This holds for any  $l$ .

Thus, for the Daubechies'  $K = 3$  wavelets, finite linear combinations of the scaling basis functions  $\phi_{kn}(x)$  can locally pointwise represent polynomials of degree two, whereas the wavelet basis functions  $\psi_{kn}(x)$  are orthogonal to degree-two polynomials.

Equation (19) implies that the projection  $P_k$  of a function  $f(x)$  on  $\mathcal{V}_k$  can be represented by

$$P_k f(x) = \sum_n a_n \phi_{kn}(x), \quad a_n = \int f(x) \phi_{kn}(x) dx, \quad (20)$$

or, equivalently,

$$P_k f(x) = \sum_n b_n \phi_{k+m,n}(x) + \sum_{k'=k+1}^{k+m} \sum_n c_{k'n} \psi_{k',n}, \quad (21)$$

$$b_n = \int f(x) \phi_{k+m,n}(x) dx, \quad c_{kn} = \int f(x) \psi_{kn}(x) dx. \quad (22)$$

For a sufficiently fine resolution (large  $-k$ ) the scaling basis functions  $\phi_{kn}(x)$  have small support and integrate to the  $n$ -independent constant  $2^{k/2}$ . If  $f(x)$  varies slowly on the support of the  $\phi_{kn}(x)$  [intervals of width  $(2K - 1)2^k$ ], then the expansion coefficients  $a_n$  are well approximated by an evaluation of  $f(x)$  at any point in the support of  $\phi_{kn}(x)$  and multiplication by  $2^{k/2}$ . This implies that the scaling function basis coefficients  $a_n$  are well approximated, up to a fixed multiplicative constant, by a sampling of the original function at points separated by  $2^k$ . These coefficients play the role of the raw image in a digital photograph. They provide an accurate, but inefficient, approximation of the function  $f(x)$ .

In representation (21), if  $f(x)$  can be accurately approximated by a polynomial of degree  $K - 1$  on the support of  $\psi_{kn}(x)$ , then  $c_{kn} \approx 0$ . This means that if  $f(x)$  can be well approximated by a low-degree local polynomial on intervals of width  $(2K - 1)2^k$ , then the coefficients  $c_{kn}$  will be small and the function can be accurately approximated if these coefficients are replaced with zero. The mean square error of this approximation is the sum of the squares of the discarded coefficients, which can be controlled by the selection of a maximum size of the discarded coefficients. Even though most of the basis functions in representation (21) are orthogonal to low-degree polynomials, the equivalence between representations (20) and (21) means that representation (21) can still locally pointwise represent low-degree polynomials. In addition, when the inverse of the wavelet transform is applied to the approximate expansion, an approximation to  $f(x)$  in the scaling function basis is obtained.

In representation (21), the coefficients  $b_n$  give a coarse description of the function and the coefficients  $c_{kn}$  add the details on finer scales.

The scaling equation and normalization condition can be used to derive exact expressions for the moments

$$\langle x^m \rangle_{\phi_{kn}} \equiv \int \phi_{kn}(x) x^m dx, \quad (23)$$

and partial moments of the scaling function

$$\langle x^m \rangle_{\phi_{kn}[l,l']} \equiv \int_{2^{k_l}}^{2^{k_{l'}}} \phi_{kn}(x) x^m, \quad n \leq l, \quad l' \leq 2K - 1 + n, \quad (24)$$

in terms of the scaling coefficients  $h_l$ . Explicit expressions for the moments and partial moments appear in Refs. [1,2,23].

For the Daubechies'  $K$  wavelets with  $K > 1$ , the second moment of the scaling function is the square of the first moment. This means that for  $K = 3$  the first moment provides a single quadrature point that will integrate the scaling function times any second-degree polynomial exactly:

$$\int \phi(x)(a + bx + cx^2)dx = a + b\langle x \rangle_{\phi} + c\langle x \rangle_{\phi}^2. \quad (25)$$

This is called the one-point quadrature. Translating and rescaling leads to one-point quadratures for all of the scaling basis functions  $\phi_{kn}(x)$ . This is a good approximation whenever the function being integrated can be accurately approximated as a degree-two polynomial on the support of  $\phi_{kn}(x)$ . The choice of  $K = 3$  Daubechies' wavelets in Refs. [1,2] is motivated by their ability to locally pointwise represent second-degree

polynomials and to exactly integrate these local polynomials with a one-point quadrature.

In Refs. [1,2,23], the moments and the scaling equation are used to compute the singular integrals

$$L_n^{k\pm} \equiv \int dx \frac{\phi_{kn}(x)}{x \pm i\epsilon}, \quad (26)$$

to any predetermined precision.

In the applications [1,2], the integral equation is approximated by projection onto an approximation space  $\mathcal{V}_k$  with the finest resolution  $k$  dictated by the problem. This projection can be computed efficiently in scaling basis (20) by use of one-point quadrature (25) and explicit integrals (26). The resulting matrix equation is transformed by the wavelet transform into an equivalent system in wavelet basis (21). In the transformed basis the kernel of the integral equation decomposes into the sum of a sparse matrix and a small matrix. The kernel is approximated by the setting of matrix elements of the kernel that are smaller than a threshold value to zero. This results in a sparse-matrix approximation. The resulting linear system is solved by use of sparse-matrix iterative techniques, such as the complex biconjugate gradient method [24,25] used in Ref. [2]. This solution is transformed back to the scaling function representation, by use of the inverse wavelet transform, and the resulting solution is inserted back in the integral equation to construct an interpolated solution [26].

The only wavelet information used in these applications is the wavelet transform and moments of the scaling function. These can both be expressed directly in terms of the scaling coefficients  $h_l$  in Table I. The basis functions never have to be computed. This is because integrals against smooth functions can be done with the one-point quadrature and the singular integrals can be expressed in terms of integrals (26). One can evaluate the solution at any point by inserting the numerical expansion in the right-hand side of the integral equation, eliminating the basis function in the expansion by using the one-point quadrature and integrals (26).

References [1,2] demonstrate that all of these steps work as expected. These references also discuss technical issues that arise because of the treatment of end points when the equations are transformed to a finite interval, as well as the need to condition the kernel matrix in two variable integral equations.

### III. DYNAMICAL EQUATIONS

The general structure of the Faddeev-Lovelace [9,10,14] equations in a relativistic quantum theory with three particles of mass  $m$  is

$$X(p, q) = D_x(p, q) + \int_0^\infty \frac{K_{xx}(p, q; p', q', z) dp' dq'}{z - e_1(p', q') - e_2(q')} X(p', q') + \int_0^\infty \frac{K_{xy}(p, q; q', z) dq'}{z - e_b(q') - e_2(q')} Y(q'), \quad (27)$$

$$Y(q) = D_y(q) + \int_0^\infty \frac{K_{yx}(q; p', q', z) dp' dq'}{z - e_1(p', q') - e_2(q')} X(p', q') + \int_0^\infty \frac{K_{yy}(q; q', z) dq'}{z - e_b(q') - e_2(q')} Y(q'), \quad (28)$$

where

$$e_1(p, q) = \sqrt{4p^2 + 4m^2 + q^2}, \quad e_2(q) = \sqrt{m^2 + q^2}, \quad (29)$$

$$e_b = \sqrt{m_b^2 + q^2}. \quad (30)$$

These equations assume one two-body bound state with mass  $m_b$ . The quantities  $X$ ,  $Y$ ,  $K$ , and  $D$  have many channel indices. The quantity  $K$  is the smooth part of the kernel. The precise structure of the kernel and driving terms of Eqs. (27) and (28) is given by Eqs. (7.71) and (7.72) of Ref. [9].

The energy denominators in the coupled set of equations come from the spectral representation of the  $2 + 1$  resolvent operators in the kernel of the equations. This form of the equations is dictated by the structure of the interaction term in relativistic Hamiltonian dynamics [9,10]. Although the forms of the singularities in Eqs. (27) and (28) differ from the way that they occur in the conventional treatment of the nonrelativistic three-body problem, the nonrelativistic three-body equations can also be put in a similar form [27,28].

The denominators that follow  $K_{xy}$  and  $K_{yy}$  can be treated by use of the methods discussed in Ref. [1]. The denominators that follow  $K_{xx}$  and  $K_{yx}$  involve moving singularities. The methods used in [1] cannot be applied to moving singularities. The purpose of this paper is to discuss the treatment of these moving singularities by use of wavelet numerical analysis.

To use wavelet methods it is advantageous to transform these energy denominators to a form in which functions of the momentum, rather than the energy, are additive. This transformation facilitates the treatment of the moving singularity. Note that  $e_1 > e_2$  for all values of  $p$  and  $q$ . If  $E > 0$ , then  $E + e_1(p, q) - e_2(q) > 0$ . It follows that one can transform the singular denominator,

$$\frac{1}{E + i0^+ - e_1(p, q) - e_2(q)}, \quad (31)$$

to a more useful form by multiplying the numerator and denominator by the nonzero function  $E + e_1(p, q) - e_2(q)$ . This leads to the equivalent expression

$$\begin{aligned} & \frac{1}{E + i0^+ - e_1 - e_2} \\ &= \frac{E + e_1 - e_2}{E^2 + e_2^2 - 2Ee_2 - e_1^2 + i0^+(E + e_1 - e_2)} \\ &= \frac{E + e_1 - e_2}{E^2 - 3m^2 - 2E\sqrt{q^2 + m^2} - 4p^2 + i0^+}, \end{aligned} \quad (32)$$

which has the advantage in that it separates the  $p$  and  $q$  dependence. In the nonrelativistic case, the  $p$  and  $q$  dependence is already separate.

The next step is to change variables,

$$x = \eta 4p^2, \quad y = \eta 2E(\sqrt{q^2 + m^2} - m), \quad (33)$$

and define

$$z' = \eta[(E - m)^2 - 4m^2]. \quad (34)$$

The parameter  $\eta$  sets a scale and can be used to fine tune  $z'$  so it is a dyadic rational of the form  $n/2^{-k}$ . The method that

we use to evaluate the singular integrals requires that  $z'$  be a dyadic rational.

A similar variable change can be used to treat the part of the equation with the fixed singularity:

$$\begin{aligned} w &= (e_2(q) + e_b(q) - m_b - m)\eta', \\ z'' &= (E - m - m_b)\eta'. \end{aligned} \quad (35)$$

Substitutions (33), (34), and (36) lead to the following equivalent equations:

$$\begin{aligned} \bar{X}(x, y) &= \bar{D}_x(x, y) + \int_0^\infty \frac{\bar{K}_{xx}(x, y; x', y') dx' dy'}{z' - x' - y' + i0^+} \bar{X}(x', y') \\ &+ \int_0^\infty \frac{\bar{K}_{xy}(x, y; w') dw'}{z'' - w' + i0^+} \bar{Y}(w'), \end{aligned} \quad (36)$$

$$\begin{aligned} \bar{Y}(w) &= \bar{D}_y(w) + \int_0^\infty \frac{\bar{K}_{yx}(w; x', y') dx' dy'}{z' - x' - y' + i0^+} \bar{X}(x', y'') \\ &+ \int_0^\infty \frac{\bar{K}_{yy}(w; w') dw'}{z'' - w' + i0^+} \bar{Y}(w'), \end{aligned} \quad (37)$$

where

$$\bar{X}(x, y) = X[p(x), q(y)], \quad \bar{Y}(w) = Y[q(w)], \quad (38)$$

$$\bar{D}_x(x, y) = D_x[p(x), q(y)], \quad \bar{D}_y(w) = D_y[q(w)], \quad (39)$$

$$\begin{aligned} \bar{K}_{xx}(x, y; x', y') &= \eta K_{xx}(p(x), q(y); p(x'), q(y'), z) \\ &\times (E + e_1[p(x'), q(y')] - e_2[q(y')]) \left| \frac{dp}{dx'} \frac{dq}{dy'} \right|, \end{aligned} \quad (40)$$

$$\bar{K}_{xy}(x, y; w) = \eta' K_{xy}(p(x), q(y); q(w), z) \times \left| \frac{dq}{dw} \right|, \quad (41)$$

$$\begin{aligned} \bar{K}_{yx}(w; x, y) &= \eta K_{yx}[q(w); p(x), q(y), z] \\ &\times (E + e_1[p(x), q(y)] - e_2[q(y)]) \left| \frac{dp}{dx} \frac{dq}{dy} \right|, \end{aligned} \quad (42)$$

$$\bar{K}_{yy}(w; w') = \eta' K_{yy}(q(w); q(w'), z'') \times \left| \frac{dq}{dw'} \right|. \quad (43)$$

Approximations are derived by use of projection methods. We seek a solution  $\bar{X}$  in the  $x$  and  $y$  variables on the approximation space  $\mathcal{V}_k \otimes \mathcal{V}_k$  and  $\bar{Y}$  in the  $w$  variables on  $\mathcal{V}_k$ . We obtain approximate equations by projecting the smooth part of the kernel and the driving on this space. We use the following approximations:

$$\bar{X}(x, y) \approx \sum_{mn} \phi_{km}(x) \phi_{kn}(y) \bar{X}_{m,n}, \quad (44)$$

$$\bar{Y}(w) \approx \sum_m \phi_{km}(w) \bar{Y}_m, \quad (45)$$

$$\bar{D}_x(x, y) \approx \sum_{mn} \phi_{km}(x) \phi_{kn}(y) \bar{D}_{m,n}, \quad (46)$$

$$\bar{D}_y(w) \approx \sum_{mn} \phi_{km}(w) \bar{D}_m, \quad (47)$$

$$\begin{aligned} \bar{K}_{xx}(x, y; x', y') &\approx \sum_{mnm'n'} \phi_{km}(x) \phi_{kn}(y) \bar{K}_{m,n;m',n'} \phi_{km'}(x') \phi_{kn'}(y'), \end{aligned} \quad (48)$$

$$\bar{K}_{xy}(x, y; w) \approx \sum_{mnl} \phi_{km}(x)\phi_{kn}(y)\bar{K}_{m,n;l}\phi_{kl}(w), \quad (49)$$

$$\bar{K}_{yx}(x, y; x', y') \approx \sum_{mm'n'} \phi_{km}(w)\bar{K}_{m;m',n'}\phi_{km'}(x')\phi_{kn'}(y'), \quad (50)$$

$$\bar{K}_{yx}(w; x, y) \approx \sum_{mnl} \phi_{kl}(w)\bar{K}_{l;mn}\phi_{km}(x)\phi_{kn}(y), \quad (51)$$

where

$$\bar{D}_{m,n} \equiv 2^k \bar{D}_x(x_m, x_n), \quad \bar{D}_m \equiv 2^{k/2} \bar{D}_y(x_m), \quad (52)$$

$$\bar{K}_{m,n;m',n'} \equiv 2^{2k} \bar{K}_{xx}(x_m, x_n; x_{m'}, x_{n'}), \quad (53)$$

$$\bar{K}_{m;m',n'} \equiv 2^{3k/2} \bar{K}_{yx}(x_m; x_{m'}, x_{n'}), \quad (54)$$

$$\bar{K}_{m,n;m'} \equiv 2^{3k/2} \bar{K}_{xy}(x_m, x_n; x_{m'}), \quad (55)$$

$$\bar{K}_{m;m'} \equiv 2^k \bar{K}_{yy}(x_m; x_{m'}) \quad (56)$$

are evaluated at the one-point quadrature points associated with  $\phi_{km}(x)$ :

$$x_m = 2^k(\langle x \rangle_\phi + m), \quad \langle x \rangle_\phi = \frac{1}{\sqrt{2}} \sum_{l=1}^{2K-1} lh_l. \quad (57)$$

The one-point quadrature formula reduces the projection to the evaluation of the kernel or driving terms at a point.

To cleanly separate the contribution from the singular integral and the dynamics it is useful to replace the product of the expansion of the solution and the expansion of the smooth part of the kernel with a single expansion of the product of these expressions. This is equivalent to the approximation

$$\phi_{km}(x)\phi_{kn}(x) \approx \sum_l I_{mnl}^k \phi_{kl}(x). \quad (58)$$

Although one can make the error in this approximation small as desired by choosing a sufficiently fine resolution, there is normally no need to increase the resolution.

Because the Daubechies'  $K = 3$  basis functions can locally pointwise represent second-degree polynomials, the product of two expansions in these basis functions can, at best, locally pointwise represent fourth-degree polynomials. To test this approximation, we compare the expansion of  $x^4$  with the Daubechies'  $K = 3$  basis functions to the product of expansions of  $x^2$  by using Daubechies'  $K = 3$  wavelets at a fixed resolution  $k$ . We write

$$x^2 = \sum_n x_n^2 \phi_{kn}(x), \quad (59)$$

which gives

$$x^4 = \sum_{mn} x_m^2 x_n^2 \phi_{km}(x)\phi_{kn}(x). \quad (60)$$

The expansion coefficients  $x_n^2$  in Eq. (60) are the squares of the one-point quadrature points [Eq. (57)]. With these coefficients, expression (60) is exact for the Daubechies'  $K = 3$  wavelets.

We approximate  $x^4$  by using approximation (58) in Eq. (60). The expansion coefficients

$$c_l = \int x^4 \phi_{kl}(x) dx = \sum_{mn} x_m^2 x_n^2 I_{mnl}^k \quad (61)$$

TABLE II. Test of double expansion (63).

$x$	$x^4$	$\sum x_m^2 x_n^2 I_{mnl}^k \phi_{kl}$
$-1.000000 \times 10^1$	$1.000000 \times 10^4$	$1.000000 \times 10^4$
$-9.000000$	$6.561000 \times 10^3$	$6.561000 \times 10^3$
$-8.000000$	$4.096000 \times 10^3$	$4.096000 \times 10^3$
$-7.000000$	$2.401000 \times 10^3$	$2.401000 \times 10^3$
$-6.000000$	$1.296000 \times 10^3$	$1.296000 \times 10^3$
$-5.000000$	$6.250000 \times 10^2$	$6.250002 \times 10^2$
$-4.000000$	$2.560000 \times 10^2$	$2.560002 \times 10^2$
$-3.000000$	$8.100000 \times 10^1$	$8.100015 \times 10^1$
$-2.000000$	$1.600000 \times 10^1$	$1.600010 \times 10^1$
$-1.500000$	5.062500	5.062574
$-1.000000$	1.000000	1.000050
$-5.000000 \times 10^{-1}$	$6.250000 \times 10^{-2}$	$6.252593 \times 10^{-2}$
$-3.750000 \times 10^{-1}$	$1.977539 \times 10^{-2}$	$1.979528 \times 10^{-2}$
$-2.500000 \times 10^{-1}$	$3.906250 \times 10^{-3}$	$3.920094 \times 10^{-3}$
$-1.250000 \times 10^{-1}$	$2.441406 \times 10^{-4}$	$2.519414 \times 10^{-4}$
0.000000	0.000000	$1.757732 \times 10^{-6}$
$1.250000 \times 10^{-1}$	$2.441406 \times 10^{-4}$	$2.398553 \times 10^{-4}$
$2.500000 \times 10^{-1}$	$3.906250 \times 10^{-3}$	$3.895922 \times 10^{-3}$
$3.750000 \times 10^{-1}$	$1.977539 \times 10^{-2}$	$1.975902 \times 10^{-2}$
$5.000000 \times 10^{-1}$	$6.250000 \times 10^{-2}$	$6.247759 \times 10^{-2}$
1.000000	1.000000	$9.999534 \times 10^{-1}$
2.000000	$1.600000 \times 10^1$	$1.599991 \times 10^1$
3.000000	$8.100000 \times 10^1$	$8.099986 \times 10^1$
4.000000	$2.560000 \times 10^2$	$2.559998 \times 10^2$
5.000000	$6.250000 \times 10^2$	$6.249998 \times 10^2$
6.000000	$1.296000 \times 10^3$	$1.296000 \times 10^3$
7.000000	$2.401000 \times 10^3$	$2.401000 \times 10^3$
8.000000	$4.096000 \times 10^3$	$4.096000 \times 10^3$
9.000000	$6.561000 \times 10^3$	$6.561000 \times 10^3$
$1.000000 \times 10^1$	$1.000000 \times 10^4$	$1.000000 \times 10^4$

can be expressed in terms of the integrals

$$I_{lmn}^k \equiv \int \phi_{kl}(x)\phi_{km}(x)\phi_{kn}(x) dx, \quad (62)$$

which are computed exactly in Sec. IV. The resulting approximation is

$$x^4 \approx \sum_{mnl} x_m^2 x_n^2 I_{mnl}^k \phi_{kl}(x). \quad (63)$$

The  $\phi_{kl}(x)$  are evaluated at dyadic rationals to eliminate the error in computing the scaling basis functions. The only source of error is approximation (63). Table II compares the right- and left-hand sides of approximation (63) for resolution  $k = -5$ .

At this resolution ( $k = -5$ ) the expansion is essentially exact, except near  $x = 0$ , where  $x^4$  has three vanishing derivatives. The accuracy near the critical point,  $x = 0$ , can be improved by use of a higher resolution; however, a degenerate (three vanishing derivatives) critical point is not generic.

This additional approximation gives

$$\begin{aligned} \bar{K}_{xx}(x, y; x', y') \bar{X}(x', y') \\ \approx \sum \phi_{km}(x)\phi_{kn}(y)\bar{K}_{m,n;m',n'} I_{n'n''n'''}^k I_{m'm''m'''}^k \\ \times \bar{X}_{m'',n''}\phi_{km''}(x')\phi_{kn''}(y') \end{aligned} \quad (64)$$

and similar expressions for  $\bar{K}_{yx}(w; x', y')\bar{X}(x', y')$ ,  $\bar{K}_{xy}(x, y; w')\bar{Y}(w')$ , and  $\bar{K}_{yy}(w; w')\bar{Y}(w')$ . Even though this introduces two additional sums, most of the terms are zero because  $I_{m,m',m''}^k = 0$  unless  $|m - m'|$ ,  $|m' - m''|$ , and  $|m'' - m|$  are all less than  $2K - 1$ . In Sec. IV we show that the integrals  $I_{mm'm''}^k$  can all be computed analytically by using the scaling equation.

With these approximations, the dynamical equations reduce to the following algebraic system:

$$\bar{X}_{m,n} = \bar{D}_{m,n} + \sum \bar{K}_{m,n;m',n'} I_{m''m'm''}^k I_{n''n'n''}^k J_{m''m'',n''}^k(z) \bar{X}_{m'',n''} + \sum \bar{K}_{m,n;m'} I_{m''m'm''}^k L_{m''m''}^k(z) \bar{Y}_{m''}, \quad (65)$$

$$\bar{Y}_m = \bar{D}_m + \sum \bar{K}_{m;m',n'} I_{m''m'm''}^k I_{n''n'n''}^k J_{m''m'',n''}^k(z) \bar{X}_{m'',n''} + \sum \bar{K}_{m;m'} I_{m''m'm''}^k L_{m''m''}^k(z) \bar{Y}_{m''}, \quad (66)$$

where

$$J_{m,n}^k(z) \equiv \int_0^\infty dx dy \frac{\phi_{km}(x)\phi_{kn}(y)}{z - x - y + i0^+}, \quad (67)$$

$$L_m^k(z) \equiv \int_0^\infty dx \frac{\phi_{km}(x)}{z - x + i0^+}. \quad (68)$$

Equations (65) and (66) separate the smooth part of the physics input in  $\bar{D}$  and  $\bar{K}$  from the singular part of this equation, contained in the integrals  $J_{mn}^k(z)$  and  $L_m^k(z)$ . Although the construction of the smooth kernel in the relativistic case is considerably more complicated than in the nonrelativistic case [9,10,14], given the driving term and smooth kernel, one can calculate the projections  $\bar{K}_{m,n;m',n'}$  and  $\bar{D}_{m,n}(x', y')$  by evaluating the exact driving term and kernel at the one-point quadrature point for each  $\phi_{km}(x)$ . This reduces a Galerkin projection to a simple function evaluation.

In the next section we discuss the evaluation of the integrals

$$I_{l,m,n}^k \quad \text{and} \quad J_{m,n}^k(z) \quad (69)$$

that appear in Eqs. (65) and (66). The computation of the integrals  $L_m^k(z)$  is discussed in Ref. [1]. The integrals  $I_{l,m,n}^k$ ,  $J_{m,n}^k(z)$ , and  $L_m^k(z)$  can be evaluated and stored before calculation. They are the wavelet input to the calculation. They replace all of the integrations in the integral equations and they are *independent* of the choice of dynamical model. The physics input is contained in the matrices  $\bar{K}$  and  $\bar{D}$ . Equations (65) and (66) give a clean and stable separation of the physics and the treatment of the moving singularity, which is contained in the integrals  $J_{m,n}^k(z)$ .

Equations (65) and (66) are an infinite set of equations. They can be reduced to a finite set by the inclusion of high-momentum cutoffs or transformation to a finite interval. The treatment of end points in the evaluations of  $\bar{K}$  and  $\bar{D}$  is identical to the treatment used in Refs. [1,2], in which partial moments of the scaling function are used to construct simple quadratures that exactly integrate the product of the scaling function and degree  $K - 1$  polynomials over a subinterval of the support of the scaling function [29–31]. The treatment of end points in the evaluation of  $I_{nk}^m$  and  $J_{m,n}(z)$  is discussed in Sec. IV.

Even with the reduction to a finite set of equations, the system of equations is large. It can be reduced by performing a wavelet transform on the scaling function basis. This can be

done with the method used in Refs. [2,24], which maps the interval to a circle to treat end points. This does not change the final result because the resulting transformation is still a finite orthogonal transformation.

The next step is to discard the small matrix elements in the transformed kernel and to solve the resulting equation.

As discovered in Ref. [2], the treatment of the end points leads to an ill-conditioned matrix. This is because the right tail of the scaling function is small (see Fig. 1). Some of the overlap integrals with support containing the left end point replace the orthogonality integrals by integrals of products of scaling functions over an interval in which the product is small. This can be fixed by use of the conditioning method that was used in Ref. [2]. The resulting conditioned equations are stable and can be accurately solved by use of sparse-matrix techniques.

The resulting solution can be transformed back to the scaling function basis. An interpolated solution is then constructed from the solution  $\bar{X}_{m,n}(x, y)$  of the algebraic equations by use of the Sloan interpolation method [26]:

$$\bar{X}(x, y) = \bar{D}_x(x, y) + \sum \bar{K}_{m',n'}(x, y) I_{m''m'm''}^k I_{n''n'n''}^k J_{m''m'',n''}^k(z) \bar{X}_{m'',n''} + \sum \bar{K}_{m'}(x, y) I_{m''m'm''}^k L_{m''m''}^k(z) \bar{Y}_{m''}, \quad (70)$$

$$\bar{Y}(w) = \bar{D}_y(w) + \sum \bar{K}_{m',n'}(w) I_{m''m'm''}^k I_{n''n'n''}^k J_{m''m'',n''}^k(z) \bar{X}_{m'',n''} + \sum \bar{K}_{m'}(w) I_{m''m'm''}^k L_{m''m''}^k(z) \bar{Y}_{m''}, \quad (71)$$

where

$$\bar{K}_{m',n'}(x, y) \equiv 2^k \bar{K}_{xx}(x, y; x_{m'}, x_{n'}), \quad (72)$$

$$\bar{K}_{m',n'}(w) \equiv 2^k \bar{K}_{yx}(w; x_{m'}, x_{n'}), \quad (73)$$

$$\bar{K}_{m'}(x, y) \equiv 2^{k/2} \bar{K}_{xy}(x, y; x_{m'}), \quad (74)$$

$$\bar{K}_{m'}(w) \equiv 2^{k/2} \bar{K}_{yy}(w; x_{m'}). \quad (75)$$

The basis functions never have to be evaluated to compute the input to Eqs. (65), (66), (70), and (71). These equations, along with the methods for computing integrals (69), are the main results of this paper.

#### IV. EVALUATION OF INTEGRALS

In this section we use scaling equation (1) and normalization condition (2) to evaluate the integrals  $I_{l,n,m}^k$  and  $J_{mn}^k(z)$  that appear in Eqs. (65) and (66). These integrals are defined in Eqs. (62) and (67).

The evaluation of these integrals involves the following steps:

- (i) Expressing the scale  $k$  integrals in terms of the scale  $k = 0$  integrals.
- (ii) Using the scaling equation and the normalization condition to derive a finite set of linear equations for the corresponding integrals on the infinite interval; solving the equations.
- (iii) Using the scaling equation and support conditions to construct a finite set of linear equations relating the integrals on the semi-infinite interval to those on the infinite interval; solving the equations.

The first step is to express the scale  $k$  integrals in terms of the scale 0 integrals. Using definition (10) in Eqs. (62) and (67) we obtain the relations

$$I_{l,n,m}^k = 2^{-k/2} I_{l,n,m}^0, \quad (76)$$

$$J_{mn}^k(z) = J_{mn}^0(2^{-k}z). \quad (77)$$

In applications,  $k$  is a negative integer so we can choose  $2^{-k}z$  as an integer, which is equivalent to choosing  $z$  to be a dyadic rational. We can do this for any  $E$  by adjusting the parameter  $\eta$  in Eqs. (33). As a result, it is enough to evaluate  $J_{m,n}^0(l)$  and  $I_{l,m,n}^0$  for  $l, m, n$  integers. In what follows, we define

$$I_{l,m,n} \equiv I_{l,m,n}^0, \quad (78)$$

$$J_{m,n}(k) \equiv J_{m,n}^0(k). \quad (79)$$

Both  $I_{l,n,m}$  and  $J_{m,n}(k)$  involve integrals over the half-infinite interval. The second step of our calculation is to first evaluate the corresponding integrals over the infinite interval:

$$\bar{I}_{l,n,m} = \int_{-\infty}^{\infty} \phi(x-l)\phi(x-n)\phi(x-m)dx, \quad (80)$$

$$\bar{J}_{m,n}(k) = \int_{-\infty}^{\infty} dx \int_{-\infty}^{\infty} dy \frac{\phi(x-m)\phi(y-n)}{k-x-y+i0^+}. \quad (81)$$

These integrals are easier to compute because of the simplified boundary conditions.

We do steps (2) and (3) first for the integrals  $I_{l,m,n}$  and then for the integrals  $J_{m,n}(k)$ .

To compute the integrals  $\bar{I}_{l,m,n}$  defined in definition (80), note that this definition implies that

$$\bar{I}_{l,m,n} = \bar{I}_{0,m-l,n}, \quad (82)$$

which allows us to express  $\bar{I}_{l,m,n}$  in terms of  $\bar{I}_{n,m}$ , defined by

$$\bar{I}_{m,n} = I_{0,m,n} = \int_{-\infty}^{\infty} dx \phi(x)\phi(x-m)\phi(x-n). \quad (83)$$

Because the support of  $\phi(x)$  is contained in the interval  $[0, 2K - 1]$ , there are only a finite number of nonzero values of  $\bar{I}_{m,n}$ . These have  $-2K + 2 \leq m, n \leq 2K - 2$ , and  $|m - n| < 2K - 1$ . For  $K = 3$  there are 81  $\bar{I}_{m,n}$  with  $-4 \leq m, n \leq 4$ . Sixty-one of these terms are nonzero.

We can derive linear equations that relate these integrals by using the scaling equation in the form

$$\phi(x) = \sqrt{2} \sum_{l=0}^{2K-1} h_l \phi(2x - l). \quad (84)$$

Using Eq. (84) in definition (83) gives the scaling equation for the integrals  $\bar{I}_{mn}$ :

$$\bar{I}_{m,n} = \sqrt{2} \sum_{l_m, l_n, l_k=0}^{2K-1} h_{l_k} h_{l_m} h_{l_n} \bar{I}_{2m+l_m-2l_k, 2n+l_n-l_k}. \quad (85)$$

These are homogeneous equations relating the nonzero values of  $\bar{I}_{m,n}$ . An additional inhomogeneous equation is needed to solve for the nonzero values of  $\bar{I}_{m,n}$ . The needed equation follows from normalization condition (2) and the identity

$$\sum_n \phi(x - n) = 1, \quad (86)$$

which, when used in Eq. (83), gives the inhomogeneous equations

$$\sum_{m=-2K+2}^{2K-2} \bar{I}_{m,n} = \delta_{n0}. \quad (87)$$

Equations (85) and (87) are a finite system of  $(4K - 3)$   $(4K - 3)$  linear equations that can be solved for the nonzero values of  $\bar{I}_{mn}$ . The result of these calculations of  $\bar{I}_{mn}$  with  $K = 3$  are given in Table III. The computed values of  $\bar{I}_{mn}$  can be used in Eq. (82) to obtain  $\bar{I}_{l,m,n}$  for all  $l, m$ , and  $n$ .

The last step is to use  $\bar{I}_{l,m,n}$  to compute  $I_{l,m,n}$ . The support of the scaling functions implies that if any of  $l, m$ , or  $n$  are

TABLE III.  $\bar{I}_{mn}$ ,  $K = 3$  overlap integrals (83).

$m$	$n$	$\bar{I}_{mn}$	$m$	$n$	$\bar{I}_{mn}$
-4	-4	$1.160637 \times 10^{-7}$	1	0	$1.469238 \times 10^{-1}$
-3	-4	$9.788805 \times 10^{-7}$	2	0	$7.027929 \times 10^{-3}$
-2	-4	$-2.811543 \times 10^{-6}$	3	0	$2.025919 \times 10^{-4}$
-1	-4	$6.184412 \times 10^{-6}$	4	0	$1.160637 \times 10^{-7}$
0	-4	$-4.467813 \times 10^{-6}$	-4	1	0.000000
1	-4	0.000000	-3	1	$6.184412 \times 10^{-6}$
2	-4	0.000000	-2	1	$1.159627 \times 10^{-3}$
3	-4	0.000000	-1	1	$-3.047012 \times 10^{-2}$
4	-4	0.000000	0	1	$1.469238 \times 10^{-1}$
-4	-3	$9.788805 \times 10^{-7}$	1	1	$-8.660587 \times 10^{-2}$
-3	-3	$2.025919 \times 10^{-4}$	2	1	$-3.047012 \times 10^{-2}$
-2	-3	$-5.444572 \times 10^{-4}$	3	1	$-5.444572 \times 10^{-4}$
-1	-3	$1.159627 \times 10^{-3}$	4	1	$9.788805 \times 10^{-7}$
0	-3	$-8.249248 \times 10^{-4}$	-4	2	0.000000
1	-3	$6.184412 \times 10^{-6}$	-3	2	0.000000
2	-3	0.000000	-2	2	$-2.811543 \times 10^{-6}$
3	-3	0.000000	-1	2	$-5.444572 \times 10^{-4}$
4	-3	0.000000	0	2	$7.027929 \times 10^{-3}$
-4	-2	$-2.811543 \times 10^{-6}$	1	2	$-3.047012 \times 10^{-2}$
-3	-2	$-5.444572 \times 10^{-4}$	2	2	$2.283264 \times 10^{-2}$
-2	-2	$7.027929 \times 10^{-3}$	3	2	$1.159627 \times 10^{-3}$
-1	-2	$-3.047012 \times 10^{-2}$	4	2	$-2.811543 \times 10^{-6}$
0	-2	$2.283264 \times 10^{-2}$	-4	3	0.000000
1	-2	$1.159627 \times 10^{-3}$	-3	3	0.000000
2	-2	$-2.811543 \times 10^{-6}$	-2	3	0.000000
3	-2	0.000000	-1	3	$9.788805 \times 10^{-7}$
4	-2	0.000000	0	3	$2.025919 \times 10^{-4}$
-4	-1	$6.184412 \times 10^{-6}$	1	3	$-5.444572 \times 10^{-4}$
-3	-1	$1.159627 \times 10^{-3}$	2	3	$1.159627 \times 10^{-3}$
-2	-1	$-3.047012 \times 10^{-2}$	3	3	$-8.249248 \times 10^{-4}$
-1	-1	$1.469238 \times 10^{-1}$	4	3	$6.184412 \times 10^{-6}$
0	-1	$-8.660587 \times 10^{-2}$	-4	4	0.000000
1	-1	$-3.047012 \times 10^{-2}$	-3	4	0.000000
2	-1	$-5.444572 \times 10^{-4}$	-2	4	0.000000
3	-1	$9.788805 \times 10^{-7}$	-1	4	0.000000
4	-1	0.000000	0	4	$1.160637 \times 10^{-7}$
-4	0	$-4.467813 \times 10^{-6}$	1	4	$9.788805 \times 10^{-7}$
-3	0	$-8.249248 \times 10^{-4}$	2	4	$-2.811543 \times 10^{-6}$
-2	0	$2.283264 \times 10^{-2}$	3	4	$6.184412 \times 10^{-6}$
-1	0	$-8.660587 \times 10^{-2}$	4	4	$-4.467813 \times 10^{-6}$
0	0	$9.104482 \times 10^{-1}$			

TABLE IV.  $I_{mnl}$ ,  $K = 3$  overlap integrals (91).

$m$	$n$	$l$	$I_{mnl}$	$m$	$n$	$l$	$I_{mnl}$
-4	-4	-4	$4.152357 \times 10^{-9}$	-2	-4	-4	$-5.085054 \times 10^{-7}$
-4	-4	-3	$1.155617 \times 10^{-7}$	-2	-4	-3	$-1.218375 \times 10^{-5}$
-4	-4	-2	$-5.085054 \times 10^{-7}$	-2	-4	-2	$5.118615 \times 10^{-5}$
-4	-4	-1	$1.750639 \times 10^{-6}$	-2	-4	-1	$-1.700711 \times 10^{-4}$
-4	-3	-4	$1.155617 \times 10^{-7}$	-2	-3	-4	$-1.218375 \times 10^{-5}$
-4	-3	-3	$2.879737 \times 10^{-6}$	-2	-3	-3	$-4.066737 \times 10^{-4}$
-4	-3	-2	$-1.218375 \times 10^{-5}$	-2	-3	-2	$1.869754 \times 10^{-3}$
-4	-3	-1	$4.070309 \times 10^{-5}$	-2	-3	-1	$-6.559712 \times 10^{-3}$
-4	-2	-4	$-5.085054 \times 10^{-7}$	-2	-2	-4	$5.118615 \times 10^{-5}$
-4	-2	-3	$-1.218375 \times 10^{-5}$	-2	-2	-3	$1.869754 \times 10^{-3}$
-4	-2	-2	$5.118615 \times 10^{-5}$	-2	-2	-2	$-8.932389 \times 10^{-3}$
-4	-2	-1	$-1.700711 \times 10^{-4}$	-2	-2	-1	$3.218428 \times 10^{-2}$
-4	-1	-4	$1.750639 \times 10^{-6}$	-2	-1	-4	$-1.700711 \times 10^{-4}$
-4	-1	-3	$4.070309 \times 10^{-5}$	-2	-1	-3	$-6.559712 \times 10^{-3}$
-4	-1	-2	$-1.700711 \times 10^{-4}$	-2	-1	-2	$3.218428 \times 10^{-2}$
-4	-1	-1	$5.627612 \times 10^{-4}$	-2	-1	-1	$-1.177691 \times 10^{-1}$
-3	-4	-4	$1.155617 \times 10^{-7}$	-1	-4	-4	$1.750639 \times 10^{-6}$
-3	-4	-3	$2.879737 \times 10^{-6}$	-1	-4	-3	$4.070309 \times 10^{-5}$
-3	-4	-2	$-1.218375 \times 10^{-5}$	-1	-4	-2	$-1.700711 \times 10^{-4}$
-3	-4	-1	$4.070309 \times 10^{-5}$	-1	-4	-1	$5.627612 \times 10^{-4}$
-3	-3	-4	$2.879737 \times 10^{-6}$	-1	-3	-4	$4.070309 \times 10^{-5}$
-3	-3	-3	$8.614462 \times 10^{-5}$	-1	-3	-3	$1.454880 \times 10^{-3}$
-3	-3	-2	$-4.066737 \times 10^{-4}$	-1	-3	-2	$-6.559712 \times 10^{-3}$
-3	-3	-1	$1.454880 \times 10^{-3}$	-1	-3	-1	$2.270045 \times 10^{-2}$
-3	-2	-4	$-1.218375 \times 10^{-5}$	-1	-2	-4	$-1.700711 \times 10^{-4}$
-3	-2	-3	$-4.066737 \times 10^{-4}$	-1	-2	-3	$-6.559712 \times 10^{-3}$
-3	-2	-2	$1.869754 \times 10^{-3}$	-1	-2	-2	$3.218428 \times 10^{-2}$
-3	-2	-1	$-6.559712 \times 10^{-3}$	-1	-2	-1	$-1.177691 \times 10^{-1}$
-3	-1	-4	$4.070309 \times 10^{-5}$	-1	-1	-4	$5.627612 \times 10^{-4}$
-3	-1	-3	$1.454880 \times 10^{-3}$	-1	-1	-3	$2.270045 \times 10^{-2}$
-3	-1	-2	$-6.559712 \times 10^{-3}$	-1	-1	-2	$-1.177691 \times 10^{-1}$
-3	-1	-1	$2.270045 \times 10^{-2}$	-1	-1	-1	$4.437037 \times 10^{-1}$

nonnegative, then

$$I_{l,m,n} = \bar{I}_{l,m,n}, \tag{88}$$

and if any of  $l, m,$  or  $n$  are less than  $-2K + 2$ , then

$$I_{l,m,n} = 0. \tag{89}$$

The nontrivial values of  $I_{l,m,n}$  correspond to the case that the indices  $l, m,$  and  $n$  satisfy

$$-2K + 2 \leq l, m, n \leq -1. \tag{90}$$

To calculate the remaining nonzero values of  $I_{lmn}$ , first observe that using Eq. (84) in Eq. (62) gives scaling equations for  $I_{k,m,n}$ :

$$I_{k,m,n} = \sqrt{2} \sum h_{l_k} h_{l_m} h_{l_n} I_{2k+l_k, 2m+l_m, 2n+l_n}. \tag{91}$$

These equations are not homogeneous equations because when any of the indices on the right-hand side of the equation are nonnegative,  $I_{k,m,n} = \bar{I}_{k,m,n} = \bar{I}_{m-k, n-k}$ , which is known input. This linear system can be solved for the nontrivial values of  $I_{k,m,n}$  associated with the values of  $k, m, n$  satisfying  $-2K + 2 \leq k, m, n \leq -1$ . For  $K = 3$  there are 64 values

of  $k, m, n$  satisfying  $-4 \leq k, m, n \leq -1$ . The results of this calculation for the  $K = 3$  case are given in Table IV.

All of the overlap integrals  $I_{lmn}^k$  that appear in Eqs. (65) and (66) can be expressed directly in terms of the values in the tables by use of relations (76), (88), and (89). The integrals in the tables can be computed once and stored.

Next we calculate the integrals  $J_{mn}(l)$ . We first compute  $\bar{J}_{mn}(l)$  defined in Eq. (81). With a change of variables,  $\bar{J}_{mn}(l)$  can be expressed in terms of a quantity with a single integer index,

$$\begin{aligned} \bar{J}_{mn}(k) &= \int_{-\infty}^{\infty} dx' \int_{-\infty}^{\infty} dy' \frac{\phi(x')\phi(y')}{k - m - n - x' - y' + i0^+} \\ &= \bar{J}_{k-m-n}, \end{aligned} \tag{92}$$

with

$$\bar{J}_n \equiv \int_{-\infty}^{\infty} dx \int_{-\infty}^{\infty} dy \frac{\phi(x)\phi(y)}{n - x - y + i0^+}. \tag{93}$$

The support  $[0, 2K - 1]$  of the scaling function implies that in this integral  $x + y$  ranges from 0 to  $4K - 2$ . This means

that for  $|n| > (4K - 2)$  the series

$$\bar{J}_n = \frac{1}{n} \sum_{k=0}^{\infty} \int_{-\infty}^{\infty} dx \int_{-\infty}^{\infty} dy \frac{1}{n^k} (x+y)^k \phi(x)\phi(y) \quad (94)$$

converges. Using the binomial theorem, we can express the integrals in this series in terms of the known moments [Eq. (23)] [1] of the scaling function

$$\bar{J}_n = \sum_{m=0}^{\infty} \sum_{k=0}^m \frac{1}{n^{m+1}} \frac{m!}{k!(m-k)!} \langle x^k \rangle \langle x^{m-k} \rangle. \quad (95)$$

If  $\bar{J}_n(N)$  is the approximation we define by summing the first  $N$  terms of series (95), it follows that

$$|\bar{J}_n - \bar{J}_n(N)| < \left[ \frac{(4K-2)}{|n|} \right]^{N+1} \frac{(2K-1)^2}{|n-4K+2|} \phi_{\max}^2, \quad (96)$$

where  $\phi_{\max}$  is the maximum value ( $< 1.5$  for  $K = 3$ ) of the scaling function. For  $|n| \gg 4K - 2$  this error can be made as small as machine accuracy for modest values of  $N$ .

Thus, for large  $|n|$ , one can compute the integrals  $\bar{J}_n$  efficiently and accurately by truncating the sum in Eq. (95). To compute the  $\bar{J}_n$  for smaller values of  $n$ , note that the  $\bar{J}_n$  for different values of  $n$  are related by scaling equation (84), which, when used in Eq. (93), gives linear scaling equations for  $\bar{J}_n$ :

$$\bar{J}_n = \sum_{l'} h_l h_{l'} \bar{J}_{2n-l-l'}. \quad (97)$$

Equation (97) can be used to calculate  $\bar{J}_n$  recursively with  $\bar{J}_m$  used for large  $|m|$  used as input. This recursion can be used to step up in negative  $n$  until  $n = -1$  and down in positive  $n$  until  $n = 4K - 1$ . This provides an efficient and accurate method for calculating all of the  $\bar{J}_n$  for  $n < 0$  and  $n > 4K - 2$ .

The remaining values,  $0 \leq n \leq 4K - 2$ , correspond to cases in which the denominator of the singular integral of Eq. (93) vanishes on the support of the integrand.

Scaling relations (97) are still satisfied for these values of  $n$ , giving  $4K - 1$  equations relating the unknown  $\bar{J}_0 \cdots \bar{J}_{4K-2}$  to the known values of  $\bar{J}_n$  for  $n < 0$  and  $n > 4K - 2$ . Unlike the equations for  $\bar{I}_{lmn}$ , these equations cannot be linearly independent because they do not specify the treatment of the singular integral. One more equation is needed.

One can derive the desired equation by observing that the integral  $\bar{J}_n$  can be expressed in terms of the autocorrelation function [32–34]  $\Phi(x)$  of the scaling function as

$$\bar{J}_n = - \int_{-\infty}^{\infty} \frac{\Phi(y)}{y-n-i0^+} dy, \quad (98)$$

where

$$\Phi(x) \equiv \int_{-\infty}^{\infty} \phi(x-y)\phi(y)dy. \quad (99)$$

This is the key result that is needed to apply wavelet numerical analysis to problems with moving singularities. The properties

$$\int \phi(x)dx = 1, \quad 1 = \sum_n \phi(x+n) \quad (100)$$

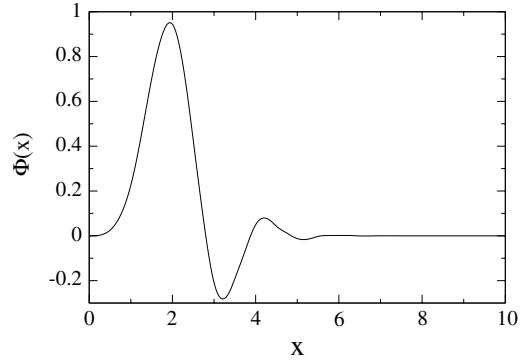


FIG. 3. Daubechies'  $K = 3$  autocorrelation function.

of the scaling function imply that the autocorrelation function satisfies

$$\int \Phi(x)dx = 1, \quad 1 = \sum_n \Phi(x+n) \quad (101)$$

and has support on  $[0, 4K - 2]$ . The autocorrelation function is plotted in Fig. 3.

Using Eq. (101) in Eq. (98) gives the additional linear constraint on the integrals  $\bar{J}_n$ :

$$\begin{aligned} -i\pi &= - \int_{-m}^m \frac{dx}{x-i0^+} \\ &= - \sum_n \int_{-m}^m dx \frac{\Phi(x+n)}{x-i0^+} \\ &= - \sum_n \int_{n-m}^{n+m} dx \frac{\Phi(x)}{x-n-i0^+}, \end{aligned} \quad (102)$$

which holds for any  $m$ . Replacing  $-i\pi$  on the left-hand side of Eq. (102) with zero gives the principal value; by  $+i\pi$  it gives the limit on the other side of the real line.

If  $m > 4K - 2$ , Eq. (102) can be expressed as

$$\begin{aligned} -i\pi &= \sum_{n=-m}^m \bar{J}_n + \sum_{n=m+1}^{m+4K-3} \int_{n-m}^{4K-2} \frac{\Phi(x)}{n-x+i0^+} dx \\ &\quad + \sum_{n=-m+1}^{-m+4K-3} \int_0^{n+m} \frac{\Phi(x)}{n-x+i0^+} dx. \end{aligned} \quad (103)$$

For  $|n| > 4K - 2$  the boundary integrals

$$\int_{n-m}^{4K-2} \frac{\Phi(x)}{n-x+i0^+} dx = \int_{n-m}^{\infty} \frac{\Phi(x)}{n-x+i0^+} dx, \quad (104)$$

$$\int_0^{n+m} \frac{\Phi(x)}{n-x+i0^+} dx = \int_{-\infty}^{n+m} \frac{\Phi(x)}{n-x+i0^+} dx \quad (105)$$

can be expanded in a convergent power series in terms of partial moments of the autocorrelation functions

$$\int_{n-m}^{4K-2} \frac{\Phi(x)}{n-x+i0^+} dx = \frac{1}{n} \sum_{k=0}^{\infty} \frac{1}{n^k} \int_{n-m}^{\infty} \Phi(x)x^k dx, \quad (106)$$

$$\int_0^{n+m} \frac{\Phi(x)}{n-x+i0^+} dx = \frac{1}{n} \sum_{k=0}^{\infty} \frac{1}{n^k} \int_{-\infty}^{n-m} \Phi(x)x^k dx. \quad (107)$$

TABLE V.  $J_{mn}$ ,  $K = 3$  singular integrals (93).

$m$	$J$	
0	$-6.400535 \times 10^{-1}$	$+i0.000000$
1	$-1.570288$	$-i7.088321 \times 10^{-1}$
2	$6.615596 \times 10^{-1}$	$-i2.966393$
3	$1.719674$	$+i6.560028 \times 10^{-1}$
4	$6.721642 \times 10^{-2}$	$-i1.554882 \times 10^{-1}$
5	$3.595012 \times 10^{-1}$	$+i3.858342 \times 10^{-2}$
6	$2.261977 \times 10^{-1}$	$-i5.023224 \times 10^{-3}$
7	$1.853414 \times 10^{-1}$	$-i4.383938 \times 10^{-4}$
8	$1.569998 \times 10^{-1}$	$-i3.586652 \times 10^{-6}$
9	$1.357112 \times 10^{-1}$	$-i4.424016 \times 10^{-9}$
10	$1.195044 \times 10^{-1}$	$+i0.000000$

The error after the series in Eq. (106) or (107) is truncated after  $N$  terms is bounded by

$$\left(\frac{4K-2}{n}\right)^{N+1} \frac{4K-2}{n-4K+2} \Phi_{\max}, \quad (108)$$

where  $\Phi_{\max} < 1$  (for  $K = 3$ ) is the maximum value of the autocorrelation function. It is easy to compute these quantities to machine accuracy. The partial moments of the autocorrelation function in Eqs. (106) and (107), which are needed as input to Eq. (103), can be computed analytically. This calculation is discussed in the appendix.

Equations (97) and (103) can be solved for  $\bar{J}_n$  for  $0 \leq n \leq 4K - 2$  in terms of left-hand side of Eq. (103), the partial moments of the autocorrelation function, and the integrals for  $|n| > 4K - 2$ . The results of these calculations are the nine complex numbers in Table V. When combined with Eq. (95), these results give us an efficient means to evaluate  $\bar{J}_m$  for all  $m$ . The solution for the principal value is given by the real values in Table V, and the conjugate of the values in the table gives the singular integral approaching the real line from the upper half-plane.

The last step is to compute the singular integrals  $J_{mn}(k)$  that appear in integral equations (65) and (66). To evaluate these quantities, first we note that  $J_{mn}(k)$  is symmetric in  $m$  and  $n$ , so we can that assume  $m \geq n$ . For  $n \geq 0$  we can express  $J_{mn}(k)$  in terms of  $\bar{J}_n$ :

$$J_{mn}(k) = \bar{J}_{k-m-n}. \quad (109)$$

When either  $m$  or  $n$  is less than  $-2K + 2$  then

$$J_{mn}(k) = 0. \quad (110)$$

The nontrivial values of  $J_{mn}(k)$  correspond to  $m$  nonnegative and  $-2K + 2 \leq n \leq -1$ , and both  $-2K + 2 \leq n, m \leq -1$ . This still includes an infinite number of integrals because  $k$  can take any value.

We discuss the treatment of  $m$  nonnegative and  $-2K + 2 \leq m \leq -1$  separately. When  $m$  is nonnegative the integral becomes

$$J_{mn}(k) = J_n(k - m), \quad (111)$$

where

$$J_n(m) \equiv \int_0^\infty dx \int_{-\infty}^\infty dy \frac{\phi(x-n)\phi(y)}{m-x-y+i0^+}. \quad (112)$$

Because in this case  $n$  is within  $2K - 2$  of zero, for large  $|m|$  we can compute this in terms of moments (23) and partial moments (24) of the scaling function by using the series method:

$$J_n(m) = \sum_l \frac{1}{(m-n)^{l+1}} \sum_{k=0}^l \langle x^k \rangle_{\phi[-n, 2K-1]} \langle x^{l-k} \rangle_{\phi}. \quad (113)$$

The error made by keeping  $N$  terms in the  $l$  sum is bounded by

$$\left(\frac{2K-1}{m-n}\right)^{N+1} \frac{(2K-1)^2}{m-n-2K+1} (\phi_{\max})^2, \quad (114)$$

which one can make as small as desired by choosing a large enough  $m$ .

Using Eq. (84) in Eq. (112) gives

$$J_n(m) = \sum_{l=0}^{2K-1} \sum_{l'=0}^{2K-1} h_l h_{l'} J_{2n+l}(2m-l'), \quad (115)$$

which relates these integrals for different values of  $m$  and  $n$ . Equation (115) can be used to recursively step down from large values of  $|m|$  to  $m = -1$  from below and  $m = 2K$  from above. Some terms in this recursion will be complex because they involve the integrals  $\bar{J}_n$  for  $1 \leq n \leq 4K - 3$ .

The values of  $J_n(m)$  that cannot be computed directly from the moments or by the recursion have  $-2K + 2 \leq n \leq -1$  and  $0 \leq m \leq 2K - 1$ . We can compute these by treating Eq. (115) as a system of linear equations for the unknown  $J_n(m)$ 's. This works because the terms in Eq. (115) include some of the previously computed integrals. The results of this calculation are shown in Table VI.

TABLE VI.  $J_m(n)$ ,  $K = 3$  singular integrals (112).

$m$	$n$	$J$	
-4	0	$-5.270534 \times 10^{-5}$	$+i0.000000$
-4	1	$1.328492 \times 10^{-4}$	$-i1.360295 \times 10^{-3}$
-4	2	$4.129155 \times 10^{-4}$	$+i3.906821 \times 10^{-4}$
4	3	$-9.487772 \times 10^{-5}$	$-i9.892161 \times 10^{-5}$
-4	4	$3.178448 \times 10^{-6}$	$-i1.800341 \times 10^{-6}$
-4	5	$1.039698 \times 10^{-7}$	$-i6.117942 \times 10^{-9}$
-3	0	$-4.625359 \times 10^{-3}$	$+i0.000000$
-3	1	$-2.620525 \times 10^{-3}$	$-i5.640861 \times 10^{-2}$
-3	2	$2.569291 \times 10^{-2}$	$+i1.368533 \times 10^{-2}$
-3	3	$-2.507103 \times 10^{-4}$	$-i2.505784 \times 10^{-3}$
-3	4	$-1.189214 \times 10^{-3}$	$-i3.325919 \times 10^{-4}$
-3	5	$8.403857 \times 10^{-5}$	$+i4.945118 \times 10^{-6}$
-2	0	$5.719523 \times 10^{-2}$	$+i0.000000$
-2	1	$8.006177 \times 10^{-2}$	$+i3.624922 \times 10^{-1}$
-2	2	$-2.606313 \times 10^{-1}$	$-i7.778517 \times 10^{-2}$
-2	3	$3.145142 \times 10^{-2}$	$+i2.488590 \times 10^{-2}$
-2	4	$-1.188904 \times 10^{-2}$	$-i5.439550 \times 10^{-3}$
-2	5	$-9.599595 \times 10^{-3}$	$-i4.332178 \times 10^{-4}$
-1	0	$-2.730099 \times 10^{-1}$	$+i0.000000$
-1	1	$-4.302964 \times 10^{-1}$	$-i1.483101$
-1	2	$1.269047$	$+i2.936519 \times 10^{-1}$
-1	3	$-2.565108 \times 10^{-1}$	$-i9.893945 \times 10^{-2}$
-1	4	$1.173431 \times 10^{-1}$	$+i4.010587 \times 10^{-2}$
-1	5	$4.476128 \times 10^{-2}$	$-i5.054775 \times 10^{-3}$

What remains are the  $J_{mn}(k)$  when both  $m$  and  $n$  fall between  $-2K + 2$  and  $-1$ . In this case, when  $|k|$  is large,  $J_{mn}(k)$  can be expressed in the form of a convergent power series in terms of moments and partial moments of the scaling function. The scaling equations can be used to step up or down in  $k$  until  $k$  is between 0 and  $2K - 1$ ; in addition they can also be used to solve for cases in which

$$-2K + 2 \leq m, \quad n \leq -1, \quad 0 \leq k \leq 2K - 1. \quad (116)$$

In a normal application the value  $k$  represents the on-shell energy. It will be large if there are a lot of basis functions with support on either side of the on-shell point. Although  $J_{mn}(k)$  can be calculated at points (116) from the values known from scaling equation (115), these points do not arise in most applications.

This completes the computation of the singular integrals that appear in Eq. (65). Although the computation is tedious, it is both stable and straightforward.

### V. CONCLUSION

In this paper we discussed the application of wavelet numerical analysis to the relativistic three-body problem. The method starts by making variable changes in the relativistic Faddeev-Lovelace equations so that the moving scattering singularity has simple scaling properties.

The next step is to project the equation in the transformed variables on a finite resolution subspace of the three-body Hilbert space. We compute the matrix representation of the integral equation in this approximation space by evaluating the driving terms and smooth part of the kernel at the one-point quadrature points. Additional integrals involving the singular part of the kernel over the basis functions are needed to compute the full kernel. These integrals can be calculated either exactly or with precisely controlled errors by use of scaling equation (1) and normalization condition (2). Methods for computing all of the required integrals are discussed in detail in Sec. IV and the appendix. Explicit values of the required integrals are computed and appear in Tables III–VI. The physics input is in the driving term and smooth part of the kernel. The integrals over the singular part of the kernel are independent of the dynamics.

The resulting system of equations in the high-resolution basis, although easy to compute, is large. The wavelet transform can then be applied to the kernel and driving terms of Eqs. (65) and (66) to transform the representations of the kernel and driving term in the high-resolution scaling basis to representations in a basis consisting of low-resolution scaling functions and wavelet basis functions with resolutions that fall between the high-resolution and the low-resolution basis. The transformation to this new basis takes  $O(N)$  steps. In the new basis the kernel can naturally be expressed as the sum of a sparse matrix and a small matrix. The key approximation is to replace the small part of the kernel with zero. One can control the size of the error made in this approximation by changing the threshold size for discarding matrix elements.

The sparse matrix can be solved by use of sparse-matrix techniques. In Ref. [2] Kessler *et al.* did this by first conditioning the matrix and then by using the complex biconjugate

gradient method. The resulting solution was transformed back to the scaling basis by use of the inverse wavelet transform. The approximation was improved when the resulting matrix solution was substituted back into the original Eq. [26]. The step has the added benefit, as seen in Eqs. (70) and (71), that the basis functions never have to be calculated. The key result that was needed to calculate integrals associated with the moving singularities is the observation by Beylkin [32] and Beylkin and Saito [33,34] that integrals of scaling functions over moving singularities can be expressed as integrals of the autocorrelation function of the scaling function over a fixed singularity. This leads to a practical and stable method for computing the integrals. The methods do not require subtractions or careful choices of quadrature points; for the Daubechies'  $K = 3$  basis they are reduced to solving a system of 11 linear equations. The required properties of the autocorrelation function are derived in the appendix.

The research in Refs. [1,2] demonstrated that the wavelet method led to sparse-matrix approximations, resulting in negligible errors. The structure of the kernel in the relativistic three-body case indicates that the wavelet method will lead to accurate sparse-matrix approximations to the relativistic Faddeev-Lovelace equations.

The increase in efficiency in this method is due to the saving in computational effort in going from solving a large dense set of linear equations to an approximately equivalent set of equations with a sparse matrix. The wavelet method will lead to a significant savings in computational effort for a large system. The method presented in this paper still starts with a large matrix. Additional savings would be possible if the matrix elements could be computed directly in the wavelet basis because the small matrix elements could be discarded without being stored. Development of an efficient method for such a direct calculation is an open problem.

Our conclusion is that wavelet numerical analysis can be used to accurately approximate the relativistic Faddeev-Lovelace equations by a linear system of equations with a sparse kernel matrix.

### ACKNOWLEDGMENTS

This work supported in part by the Office of Science of the U.S. Department of Energy, under contract DE-FG02-86ER40286. The authors acknowledge discussions with Fritz Keinert and Gerald Payne that contributed materially to this work.

### APPENDIX A

The autocorrelation function of the scaling function is defined by

$$\Phi(x) = \int_{-\infty}^{\infty} \phi(x - y)\phi(y)dy. \quad (A1)$$

Because the support of the scaling function is  $[0, 2K - 1]$ , the autocorrelation function has support  $[0, 4K - 2]$ .

Using scaling equation (84) for the scaling function in definition (A1) of the autocorrelation function leads to the scaling equation for the autocorrelation function:

$$\Phi(x) = \sum_l \sum_{l'} h_l h_{l'} \Phi(2x - l' - l). \quad (A2)$$

TABLE VII. Daubechies'  $K = 3$  autocorrelation scaling coefficients.

$a_0$	$7.825529 \times 10^{-2}$
$a_1$	$3.796160 \times 10^{-1}$
$a_2$	$6.767361 \times 10^{-1}$
$a_3$	$4.612557 \times 10^{-1}$
$a_4$	$-4.471656 \times 10^{-2}$
$a_5$	$-1.687321 \times 10^{-1}$
$a_6$	$-2.481571 \times 10^{-3}$
$a_7$	$3.922363 \times 10^{-2}$
$a_8$	$-1.563883 \times 10^{-3}$
$a_9$	$-4.256471 \times 10^{-3}$
$a_{10}$	$8.774429 \times 10^{-4}$

If we define

$$a_l = \frac{1}{\sqrt{2}} \sum_{l'=0}^{\min(l, 2K-1)} h_{l-l'} h_{l'}, \quad 0 \leq l \leq 4K - 2, \quad (\text{A3})$$

Eq. (A2) can be put in the same form as that of Eq. (1):

$$D\Phi(x) = \sum_{l=0}^{4K-2} a_l T^l \Phi(x). \quad (\text{A4})$$

The scaling coefficients  $a_k$  for the Daubechies'  $K = 3$  autocorrelation function are given in Table VII.

Normalization condition (1) of the scaling function can be used in definition (A1) of the autocorrelation function to derive the normalization condition:

$$\int \Phi(x) dx = 1. \quad (\text{A5})$$

Scaling equation (A2) and normalization condition (A5) can be used calculate moments and partial moments of the autocorrelation function. To calculate the moments of the autocorrelation function, use

$$\langle x^k \rangle_\Phi = \int \Phi(x) x^k dx, \quad (\text{A6})$$

$$\langle x^k \rangle_\Phi = \frac{1}{2^{k+1/2}} \sum_l a_l \sum_{n=0}^k \frac{k!}{n!(k-n)!} l^{n-k} \langle x^n \rangle_\Phi. \quad (\text{A7})$$

 TABLE VIII. Daubechies'  $K = 3$  autocorrelation moments.

$\langle x^0 \rangle_\Phi$	1.000000
$\langle x^1 \rangle_\Phi$	1.634802
$\langle x^2 \rangle_\Phi$	2.672579
$\langle x^3 \rangle_\Phi$	4.167773
$\langle x^4 \rangle_\Phi$	5.825913
$\langle x^5 \rangle_\Phi$	6.817542
$\langle x^6 \rangle_\Phi$	8.807917
$\langle x^7 \rangle_\Phi$	$4.055470 \times 10^1$
$\langle x^8 \rangle_\Phi$	$2.899550 \times 10^2$
$\langle x^9 \rangle_\Phi$	$1.695851 \times 10^3$
$\langle x^{10} \rangle_\Phi$	$8.321402 \times 10^3$

Moving the  $n = k$  term to the left-hand side of the equation gives recursion relation

$$\langle x^k \rangle_\Phi \equiv \frac{1}{2^k - 1} \frac{1}{\sqrt{2}} \sum_l a_l \sum_{n=1}^k \frac{k!}{n!(k-n)!} l^n \langle x^{k-n} \rangle_\Phi. \quad (\text{A8})$$

The recursion is started with normalization condition (A5). The lowest moments are tabulated in Table VIII.

The partial moments of the autocorrelation function satisfy the scaling equation

$$\begin{aligned} \langle x^k \rangle_{\Phi, [m, \infty]} &\equiv \int_m^\infty \Phi(x) x^k dx \\ &= \sum_l a_l \sum_{n=0}^k \frac{\sqrt{2}}{2^{k+1}} \frac{k!}{n!(k-n)!} l^m \langle x^{k-m} \rangle_{\Phi, [2m-l, \infty]}. \end{aligned} \quad (\text{A9})$$

When  $m \geq 4K - 2$ , these partial moments become ordinary moments whereas when  $m \leq 0$  they vanish. This gives us a linear system for partial moments in terms of the full moments and lower partial moments. These equations can be solved recursively. Partial moments corresponding to more general intervals can be computed by subtraction:

$$\langle x^k \rangle_{\Phi, [m, n]} = \langle x^k \rangle_{\Phi, [m, \infty]} - \langle x^k \rangle_{\Phi, [n, \infty]}. \quad (\text{A10})$$

[1] B. M. Kessler, G. L. Payne, and W. N. Polyzou, *Few-Body Syst.* **33**, 1 (2003).  
 [2] B. M. Kessler, G. L. Payne, and W. N. Polyzou, *Phys. Rev. C* **70**, 034003 (2004).  
 [3] See <http://www.jpeg.org>.  
 [4] V. G. J. Stoks, R. A. M. Klomp, C. P. F. Terheggen, and J. J. de Swart, *Phys. Rev. C* **49**, 2950 (1994).  
 [5] R. B. Wiringa, V. G. J. Stoks, and R. Schiavilla, *Phys. Rev. C* **51**, 38 (1995).  
 [6] R. Machleit, *Phys. Rev. C* **63**, 024001 (2001).  
 [7] S. C. Pieper and R. B. Wiringa, *Annu. Rev. Nucl. Part. Sci.* **51**, 53 (2001).  
 [8] H. Witała, J. Golak, W. Glöckle, and H. Kamada, *Phys. Rev. C* **71**, 054001 (2005).

[9] B. D. Keister and W. N. Polyzou, in *Advances in Nuclear Physics*, edited by J. W. Negele and E. W. Vogt (Plenum, New York, 1991), Vol. 20.  
 [10] W. Glöckle, T.-S. H. Lee, and F. Coester, *Phys. Rev. C* **33**, 709 (1986).  
 [11] W. N. Polyzou, *J. Math. Phys.* **43**, 6024 (2002).  
 [12] M. G. Fuda and H. Alharbi, *Phys. Rev. C* **68**, 064002 (2003).  
 [13] W. N. Polyzou, *Phys. Rev. C* **68**, 015202 (2003), [nucl-th/0302023](https://arxiv.org/abs/nlth/0302023).  
 [14] F. Coester, *Helv. Phys. Acta* **38**, 7 (1965).  
 [15] R. A. Malfliet and J. A. Tjon, *Nucl. Phys.* **A27**, 161 (1969).  
 [16] G. L. Payne, J. L. Friar, B. F. Gibson, and I. R. Afnan, *Phys. Rev. C* **22**, 823 (1980).

- [17] I. Daubechies, *Commun. Pure Appl. Math.* **XLI**, 909 (1988).
- [18] I. Daubechies, *Ten Lectures on Wavelets* (Society for Industrial and Applied Mathematics, Philadelphia, 1992).
- [19] G. Kaiser, *A Friendly Guide to Wavelets* (Birkhäuser, Boston, 1994).
- [20] H. L. Resnikoff and R. O. Wells, *Wavelet Analysis: The Scalable Structure of Information* (Springer-Verlag, New York, 1998).
- [21] G. Strang, *SIAM Rev.* **31**, 4, 614 (1989).
- [22] O. Bratelli and P. Jorgensen, *Wavelets Through a Looking Glass, The World of the Spectrum* (Birkhäuser, Boston, 2002).
- [23] B. M. Kessler, G. L. Payne, and W. N. Polyzou, *Wavelet Notes*, nucl-th/0305025.
- [24] W. H. Press, S. A. Teukolsky, W. T. Vetterling, and B. P. Flannery, *Numerical Recipes in C* (Cambridge University Press, Cambridge, 1992).
- [25] G. H. Golub and C. F. Van Loan, *Matrix Computations* (Johns Hopkins University Press, Baltimore, 1996).
- [26] I. Sloan, *Math. Comput.* **30**, 758 (1976).
- [27] B. R. Karlsson and E. M. Zeiger, *Phys. Rev. D* **11**, 939 (1975).
- [28] D. Hüber, H. Kamada, H. Witała, and W. Glöckle, *Few-Body Syst.* **16**, 165 (1994).
- [29] W.-C. Shann, in *Proceedings of the 1993 Annual Meeting of Chinese Mathematics Association* (Chiao-Tung University, 1993), available at <http://citeseer.ist.psu.edu/111590.html>
- [30] W.-C. Shann and J.-C. Yan, Tech. Rep. 9301 (Department of Mathematics, National Central University, 1993), available at <http://www.math.ncu.edu.tw/shann/Math/pre.html>
- [31] W. Sweldens and R. Piessens, *SIAM J. Numer. Anal.* **31**, 1240 (1994).
- [32] G. Beylkin, *SIAM J. Numer. Anal.* **29**, 6, 1716 (1992).
- [33] G. Beylkin and N. Saito, in *Intelligent Robots and Computer Vision XI: Biological, Neural Net, and 3D Methods*, edited by D. P. Casasent, *Proc. SPIE* 1826, 39 (1992).
- [34] N. Saito and G. Beylkin, *IEEE Trans. Signal Process.* **41**, 12, 3584 (1993).